

GEOCHEMISTRY, WEATHERING INTENSITY AND PALEO-CLIMATIC CONDITIONS OF SOILS AROUND DUMPSITES FROM IBADAN, OYO STATE, NIGERIA

Romanus A. Obasi
Department of Geology
Ekiti State University
Ado Ekiti, NIGERIA

Henry Y. Madukwe
Department of Geology
Ekiti State University
Ado Ekiti, NIGERIA

Paulinus N. Nnabo
Department of Geology
Ebonyi State University
Abakaliki, NIGERIA

Corresponding author: R.A. Obasi (romanus.obasi@eksu.edu.ng):henrymadukwe@yahoo.co.uk

ABSTRACT

In this study, the chemical compositions, intensity of weathering, and paleo climatic conditions of the soils around dumpsites at Ibadan, Oyo State, Nigeria were studied. Ten soil samples were analyzed using the Laser ablation microprobe inductively coupled plasma- mass spectrometry (La ICP-MS) for the trace and rare earth elements and X-ray fluorescence (XRF) methods for the major oxides at the Central laboratory of the Stellenbosch University, South Africa. The results showed that the chemical compositions indicated a relatively enriched SiO_2 (44.56-67.48) Wt. %, Al_2O_3 (13.54-27.70) and Fe_2O_3 (4.90-11.62) and strongly depleted K_2O (0.57-2.45). Low concentrations (values less than one) of MgO , MnO and Na_2O reflected chemical destruction under oxidizing condition during weathering. Al_2O_3 with Fe_2O_3 and TiO_2 correlated positively suggesting their occurrence in clay minerals formed from the weathering of granite. High ranges of chemical index of alteration (CIA: 81.47-96.91) and chemical index of weathering (CIW: 91.67-99.36) in the study area indicated an intensive weathering of the parent materials. Supporting high intensity of weathering are plots of CIA against Al_2O_3 , high range of PIA (90.61- 99.32%) and the low contents of CaO , K_2O and Na_2O . Low concentrations of K_2O (K-feldspar), Na_2O (Na-feldspars) and an enriched aluminous clay mineral implied serious exposure of the parent rocks to an increased chemical weathering. In the area of provenance, the plot of Na_2O versus K_2O indicated a quartz-rich zone that suggested a mixed source origin whereas a plot of TiO_2 versus Zr showed samples that plotted in both the felsic and intermediate zones, suggesting provenance from more than one source. Reconstructed paleo-climate findings based on the climofunctions indicated that during the formation of Ibadan soils, the climate was humid and warm. The low ranges of Ca (0.08-1.67) and Mn (0.05-0.2) values indicated a warm and humid climate while the average Sr/Cu ratios (1.02) showed a warm humid weather during its deposition.

Keywords: Geochemistry, K-Na feldspar, weathering intensity, provenance, paleo-climate.

INTRODUCTION

The study area lies between longitudes $3^\circ 49' \text{E}$ and $3^\circ 57' \text{E}$ and latitudes $7^\circ 20' \text{N}$ and $7^\circ 27' \text{N}$ in the South-western Nigeria. The topography of Ibadan is generally rugged with undulating landforms characterized by ridges, hills and valleys and underlain by crystalline rocks that are resistant to mechanical weathering. Ibadan has a mean temperature range of $21.42\text{-}26.42^\circ\text{C}$ yearly and mean annual rainfall of approximately 1,420 mm. The vegetation is tropical rainforest while the drainage is dendritic and characterized with unmodified stream channels flowing in the southward and east-west directions. The area is well drained during the rainy season but the tributaries dry up during the dry season. The area is usually well drained during the rainy season but

the tributaries dry up during the dry season. The main rock types underlying the dumpsite belong to the Migmatite-gneiss-quartzite complex (Rahaman, 1976, 1988) consisting of quartz, schist and migmatite gneiss, while pegmatite and quartz occur as veins in the major rocks (Figure 1). The geology of the area is generally of the basement complex rock and sedimentary rock, with rock types consisting of quartzites of metasedimentary series and migmatites complex. Amphibole and quartz schist occur in association with migmatite gneiss, granitic gneiss and Pan African Older Granite bodies around Ibadan area (Okunlola, et al., 2009). The migmatite gneiss occurs mainly as low-lying outcrops while the quartz schist forms ridges.

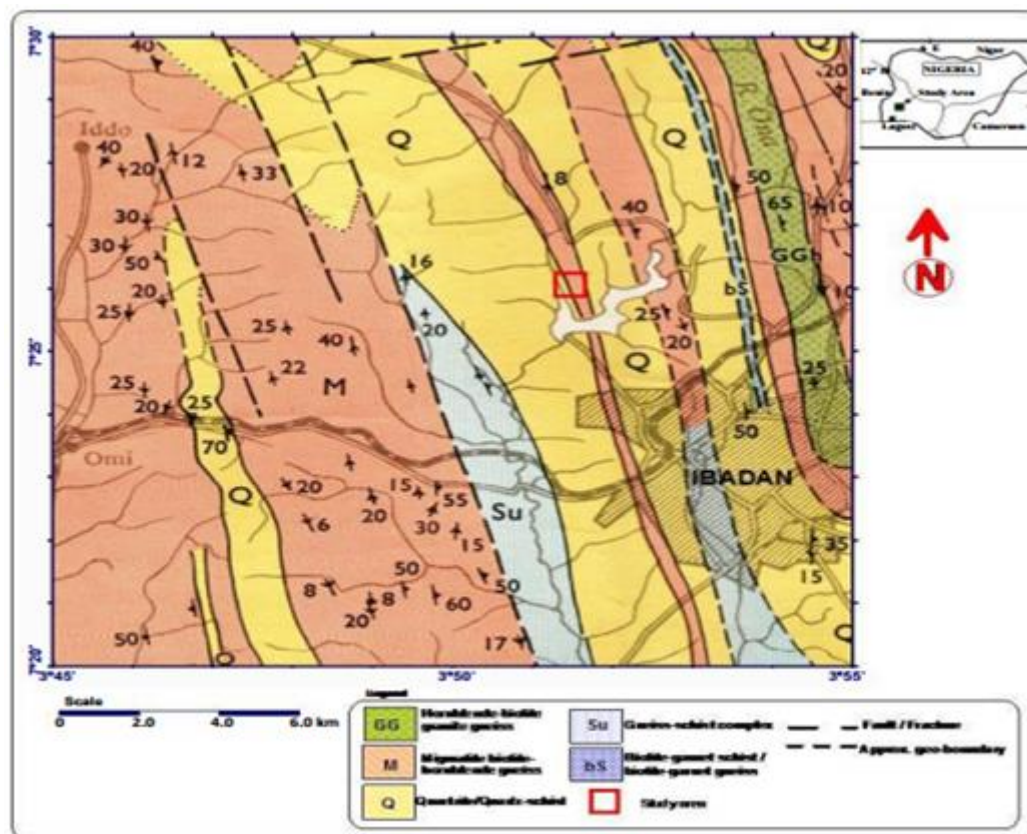


Figure 1: Map showing the geology of study area (present work).

The composition of sediments is affected by several factors such as hydraulic sizing, diagenesis, weathering and transportation processes (Taylor and McLennan 1985). The composition also depends on the primary chemical composition of the source rock materials and the tectonic setting of the depositional basins (Bhathia and Crook, 1986).

MATERIALS AND METHODS

Sample Collection

A map showing the location of the sampling points in the study area is shown in Figure 2. Ten (10) soil samples were collected with the aid of a hand auger at a depth of 0-30cm. at regular intervals. Each sample was properly immediately sealed to avoid contamination from environment and transportation.

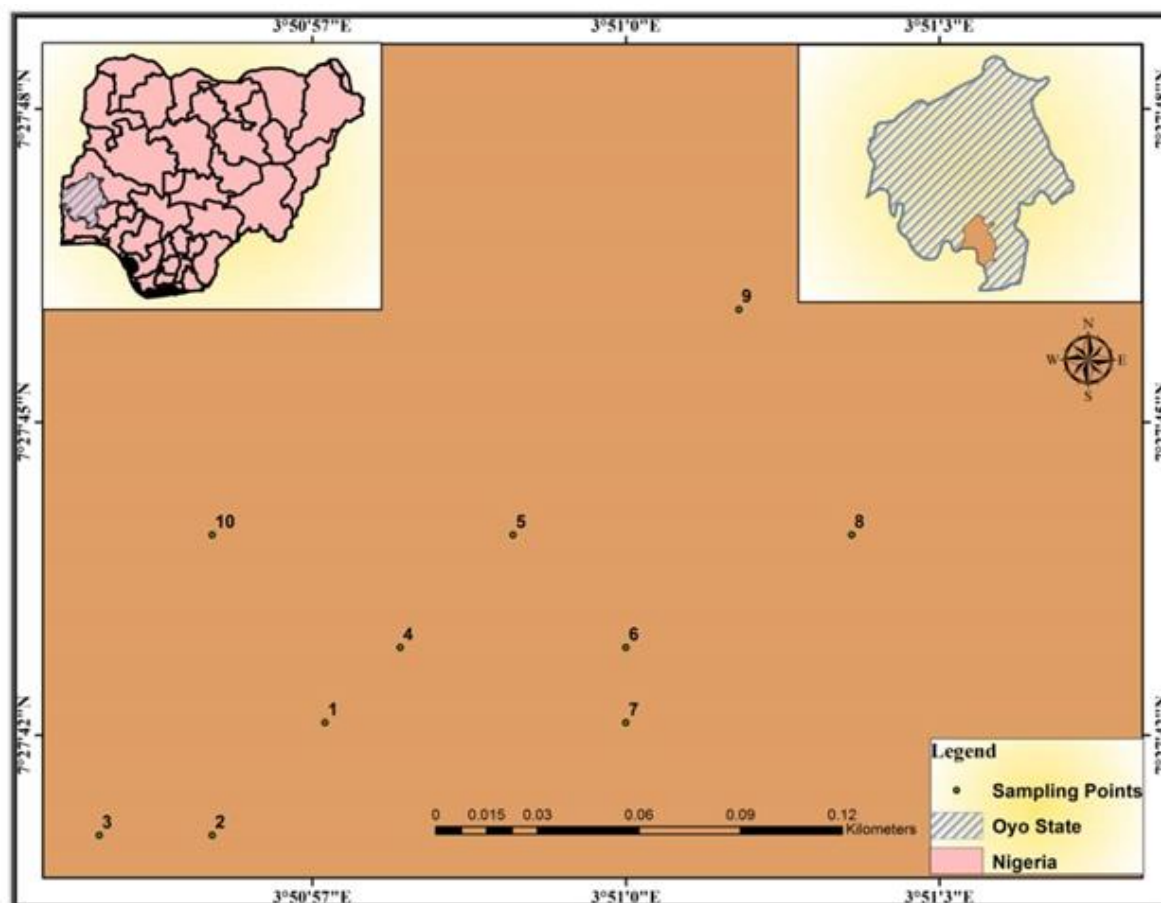


Figure 2: Map of Study Area showing the sampling points

Sample analysis

The ten soil samples were analyzed using the Laser ablation microprobe inductively coupled plasma mass spectrometry (La ICP-MS) for the trace and rare earth elements and X-ray fluorescence (XRF) methods for the major oxides (Jackson et al, 1992) at the Central laboratory of the Stellenbosch University, South Africa. The ICP-MS instrument is Perkin-Elma Sciex ELAN 5100 coupled with a UV (266 μm) laser. The laser was operated with 1 mJ/Pulse energy and 4 Hz frequency for carbonates and silicate glass. Spot diameter for these analyses is 30-50 μm . NIST 610 glass was used as a calibration standard for all the samples with ^{44}Ca as an internal standard. The analytical precision is 5% at the ppm level. Details of ICP-MS and laser operating conditions have been published by Norman et al. (1996) and Norman (1998). The results of the chemical compositions of the samples are presented in Table 1.

RESULTS AND DISCUSSIONS

The chemical compositions of the samples under study in Table 1 showed a relatively enriched SiO_2 (44.56-67.48) Wt. %, Al_2O_3 (13.54-27.70) and Fe_2O_3 (4.90-11.62) with low contents of TiO_2 (0.80-1.23) and strongly depleted K_2O (0.57-2.45). The other oxides such as MgO , MnO , and Na_2O have low concentrations that are less than one (1). The low contents of these oxides may be attributed to chemical destruction under oxidizing condition during weathering. The ratio of $\text{SiO}_2/\text{Al}_2\text{O}_3$ (1.65-4.98) shows low silica to alumina content. $\text{K}_2\text{O}/\text{Al}_2\text{O}_3$ ratio is low (0.02-0.18), an indication of low K-bearing mineral contents in relation to alumina. The low chemical ratios of $\text{Na}_2\text{O}/\text{K}_2\text{O}$ in the samples may be as a result of high degree of weathering of Na_2O rich (plagioclase) rock either at the source and/or in transit to the depositional basin (Obasi et al. 2019).

Table 1: Major oxide geochemical composition and some ratios of dumpsite soil samples

Oxides	D1	D2	D3	D4	D5	D6	D7	D8	D9	D10
SiO ₂	60.18	67.48	56.43	63.43	44.56	47.47	63.92	49.74	45.38	52.62
Al ₂ O ₃	16.73	13.54	24.00	18.85	27.70	26.49	16.93	25.42	27.56	25.49
Fe ₂ O ₃	6.98	5.06	4.90	5.86	11.62	9.99	7.66	9.98	11.56	7.45
CaO	1.37	0.43	0.31	0.18	0.15	0.08	0.13	0.13	0.15	0.23
K ₂ O	2.07	2.40	2.45	1.87	1.20	1.72	2.08	1.18	0.57	1.35
MgO	0.27	0.32	0.22	0.26	0.35	0.81	1.11	0.40	0.05	0.30
Mno	0.11	0.20	0.05	0.17	0.13	0.11	0.05	0.10	0.05	0.11
Na ₂ O	0.15	0.25	0.15	0.10	0.14	0.09	0.09	0.06	0.16	0.08
P ₂ O ₅	0.21	0.14	0.07	0.09	0.07	0.07	0.08	0.09	0.08	0.09
TiO ₂	0.80	0.79	0.78	0.97	1.21	1.19	1.09	1.23	1.11	1.01
SiO ₂ /Al ₂ O ₃	3.59	4.98	2.35	3.36	1.61	1.79	3.78	1.96	1.65	2.06
K ₂ O/Al ₂ O ₃	0.12	0.18	0.10	0.10	0.04	0.06	0.12	0.05	0.02	0.05
Na ₂ O/K ₂ O	0.07	0.10	0.06	0.05	0.12	0.05	0.04	0.05	0.28	0.06
PIA	90.61	94.25	97.91	98.38	98.92	99.32	98.54	99.22	98.90	98.73
CIA	82.33	81.47	89.19	89.76	94.90	93.34	88.04	94.89	96.91	93.89
CIW	91.67	95.22	98.12	98.54	98.96	99.36	98.72	99.26	98.89	98.80
MIA	64.67	62.94	78.37	79.52	89.79	86.68	76.08	89.77	93.81	87.70

Figure 3 shows that Al₂O₃ correlates positively with TiO₂ indicating that TiO₂ is an essential major constituent of illitic clay mineral. The positive correlation between Al₂O₃ and Fe₂O₃ shows their occurrence in clay minerals resulting from weathering of the parent rock. However, Al₂O₃ and Fe₂O₃ showed negative correlations with SiO₂. This negative trend between Al₂O₃ and SiO₂ implies that the major element composition of the samples is controlled majorly by the relative amount of quartz and aluminum clay minerals. The positive linear trend correlation between Al₂O₃ with Fe₂O₃ and TiO₂ suggest that they occur in clay minerals formed from the weathering of granite.

Weathering intensity

Nesbitt and Young (1982) and Harnois, (1988) evaluated the degree of chemical weathering/alteration of sediment source rocks and suggested that it can be determined by calculating the chemical index of alteration (CIA) in molar values is (Al₂O₃ / [Al₂O₃+CaO+Na₂+K₂O]) x 100. As the intensity of weathering increases so will Ca, Na and K decrease and work well in the index.

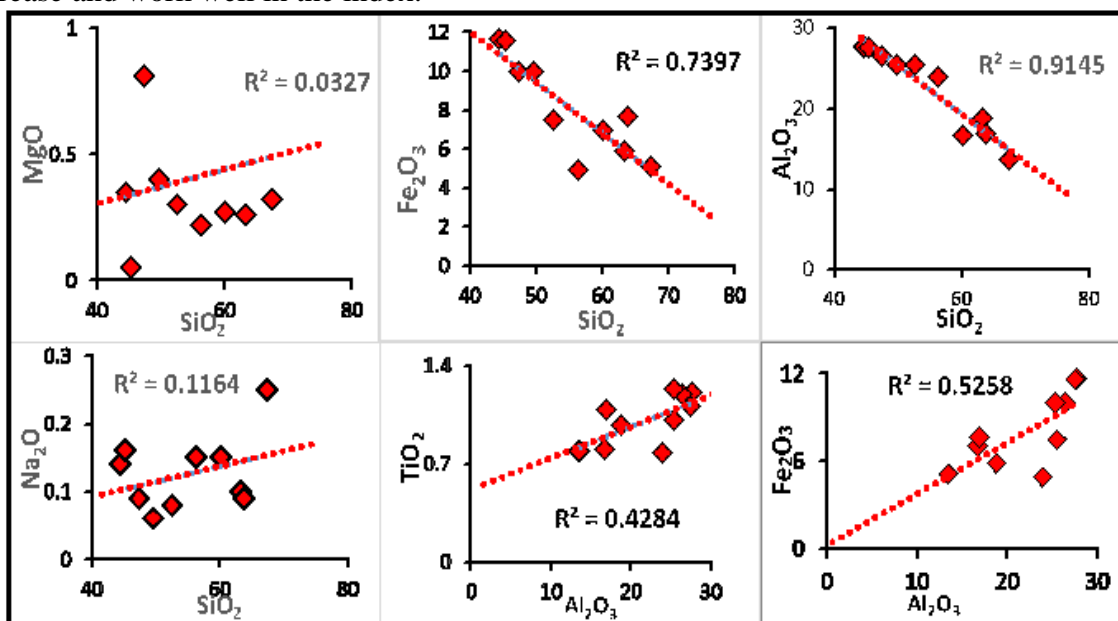


Figure 3: Cross-plots of major oxides against SiO₂ and Al₂O₃ showing the correlations

As the intensity of weathering increases so will Ca, Na and K decrease and work well in the index. McLennan, 1993 suggested the use of chemical index of weathering (CIW) which is very similar to the CIA except that it has no K_2O in the equation. The $CIW = \text{molar } (Al_2O_3 / [Al_2O_3 + CaO + Na_2O]) \times 100$. The CIA and CIW have the same interpretation such that values of 50 are taken for unweathered upper continental crust while roughly 100 is taken for highly weathered materials with complete removal of alkali and alkaline-earth elements as proposed by McLennan et al. 1983; McLennan 1993; Fedo et al. 1995; Mongelli et al. 1996. When CIAs are low with 50 or less values, they imply cool and / or arid conditions (Potter et al. 1980). The ranges of CIA and CIW of the study area are 81.47-96.91 and 91.67-99.36 respectively indicating an intensive weathering of the parent materials. The intensity of chemical weathering can also be assessed by using the plagioclase index of alteration (PIA) given in molar proportion as $PIA = (Al_2O_3 - K_2O) / [Al_2O_3 + CaO + Na_2O - K_2O] \times 100$ where CaO^* is the CaO residing in the silicate fraction (McLennan et al. 1990; Fedo et al. 1995).

Figure 4 shows a plot of CIA against Al_2O_3 indicating a high intensity of weathering in the study area. The PIA in this study area ranges between 90.61 and 99.32% indicating high degree of weathering. The high value of PIA indicated that the plagioclase in the parent rock displayed high weathering condition that resulted in low CaO, K_2O and Na_2O contents. The relatively low concentrations of K_2O (K-feldspar) and Na_2O (Na-feldspars) imply that the parent rocks have been exposed to weathering. The increase in the chemical weathering eventually leads to a depletion of the plagioclase in the parent rocks and enriched in aluminous clay minerals (Bauluz et al. 2000).

A plot of K_2O against Al_2O_3 in Figure 5 indicates vividly the clay minerals, Illite and muscovite that are susceptible to chemical weathering. This assertion played out in the increased value of Al_2O_3 (13.54-27.70) in contrast to CaO (0.43-1.37). The mineralogical index of alteration (MIA) is another weathering parameter proposed by (Voicu et al. (1997) and which is calculated as: $MIA = 2 * (MIA - 50)$. When the MIA values are between 0 and 20 % it is assumed the weathering is just starting; 20-40 % (weak); 40-60 % (moderate), and 60-100 % intense to extreme degree of weathering.

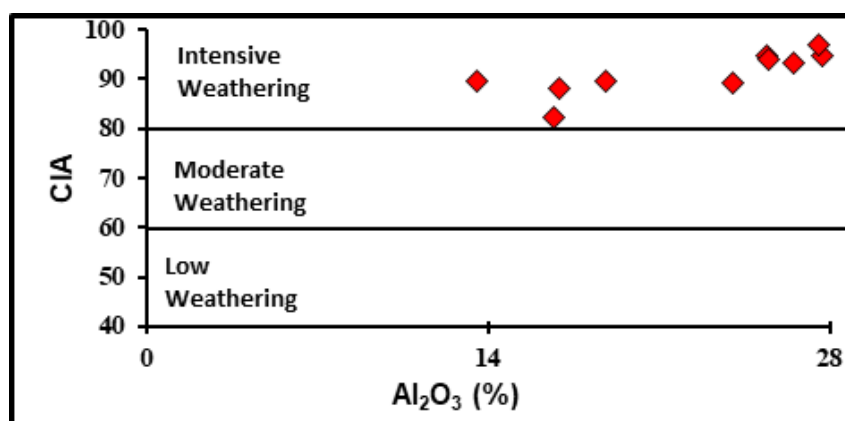


Figure 4: Plot of CIA against Al_2O_3 (Nesbitt and Young, 1982)

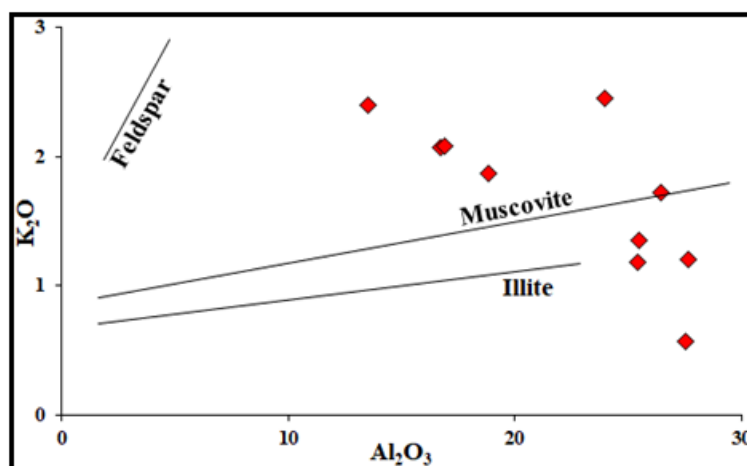


Figure 5: A plot of K_2O against Al_2O_3 (Cox et al., 1995).

The extreme value of 100% indicates complete weathering of the primary materials. The values of MIA in the study area varies from 62.94 to 93.81 % indicating that the source materials have been subjected to an intensive weathering thus affirming to the earlier results of CIW, CIA and PIA that indicated an intensive weathering of the parent materials. Table 2 is the data for trace and rare earth elements of the dumpsite soil from Ibadan, some ratios and paleoclimate indices. The ratio of SiO_2/Al_2O_3 in the study area is low (1.61-4.98) indicating that the samples have high degree of clay contents. Kaolinite clays are non-expansive and they are characterized by hot wet climate. Clay assemblages resulting from weathering reflect the pedoclimatic conditions of temperature, rainfall, vegetation, composition of the parent rock being weathered and the length of time of weathering occurrence. It is also known that the degree of weathering increases with temperature and exposure time to water and other agents of weathering. Table 1 shows that the highly mobile elements Na, K, Mg and Ca are depleted due to their leaching during the formation of clay minerals during increased chemical weathering.

Table 2: Some trace and rare earth element ratios and paleoclimate indices of the dumpsite soil from Ibadan.

Elements	D1	D2	D3	D4	D5	D6	D7	D8	D9	D10
Ba/Sr	6.35	8.16	6.60	6.99	6.00	7.92	9.61	7.52	3.36	6.60
Th/Co	1.57	1.18	2.06	2.59	0.53	1.17	2.03	1.19	2.24	1.52
La/Sc	6.57	3.91	6.55	8.61	1.64	2.52	3.99	3.09	2.64	4.37
Rb/Sr	1.28	1.61	2.21	1.99	3.44	4.91	6.22	3.7	0.87	2.93
Sr/Cu	0.11	3.64	0.86	1.82	0.67	0.79	0.51	0.76	0.76	0.28
C-value	1.81	1.52	1.56	2.45	6.30	3.70	2.24	5.61	12.35	3.78

Potter (1978) stated in the case of mineralogical maturity that low ratio of SiO_2/Al_2O_3 represents chemically immature samples. SiO_2 (quartz) contents in the soil is used in reference to the increasing sediment maturity since quartz survives preferentially to feldspar, mafic minerals and lithics (Roser and Korsch, 1986). The ratio of K_2O/Na_2O in the study area ranges from 0.02 to 0.18. Low values of SiO_2/Al_2O_3 ratios and low values of K_2O/Na_2O together indicate mineralogically immature sediment showing that the samples under study are immature. The A-CN-K ternary diagram (fig. 6) indicated the clustering of the samples at the A end suggesting high contents of aluminous clay minerals and intensive chemical weathering and transportation of the weathered materials. The samples plotted in the kaolinite, gibbsite and chlorite zone an indication of the weathered products or alteration of aluminosilicate minerals. Gibbsite is a kandite clay with a structure similar to kaolinite.

The molar proportions of Al_2O_3 (A), $CaO + Na_2O + K_2O$ (CNK) and $FeO_{tot} + MgO$ (FM) is shown in Figure 7; the diagram shows virtually all of the samples close to the A-FM line

towards the A apex, implying that there is Al enrichment and alteration of feldspars. Figure 8 shows the “kaolinisation” of the Ibadan soil samples; they are in the kaolinic and kaolinite area of the diagram, which indicates that the samples are altered to kaolinic degree. Figure 9 also shows that weathering was intense with all the samples plotting towards the SiO₂ area, which may also suggest leaching of some elements.

Kaolinite is associated with tropical soils, particularly on stable cratonic areas. This is because the intensity of weathering to form kaolinite from granite rock is greater than for other clays. Kaolinite formed through transformation reaction is less common but the existence of kaolinite interstratified with other clays suggests that these reactions can occur. Soil-formed kaolinite differs from diagenetic kaolinite in having some Fe substitution for Al, being less well ordered, and having a smaller particle size. Commercial deposits of kaolinite (china clay) have formed through metasomatic alteration of granite instead of through weathering.

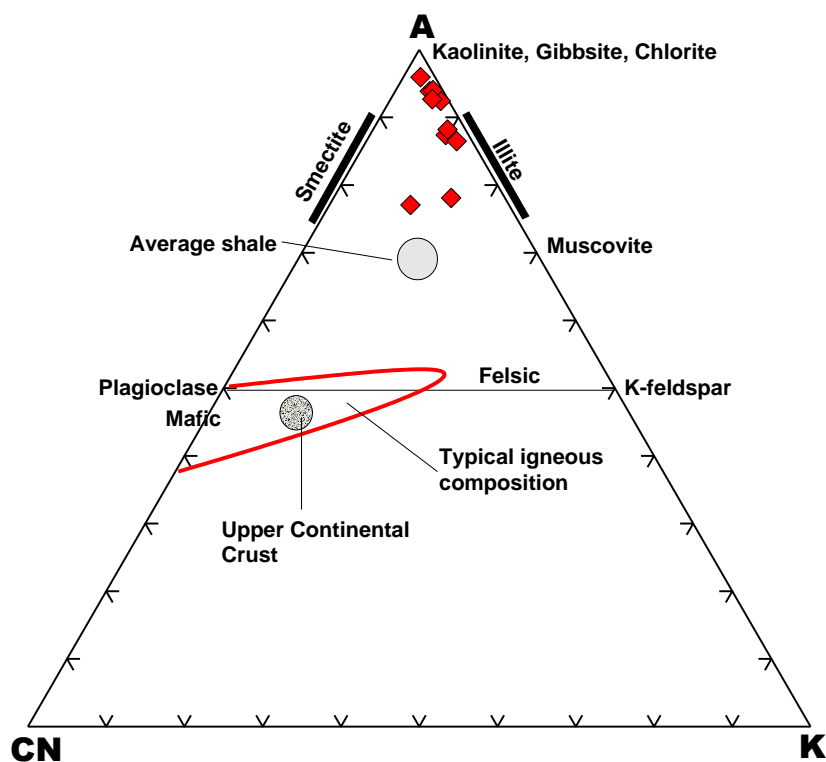


Figure 6: Ternary diagram showing the weathering trend of soil ($\text{Al}_2\text{O}_3\text{-CaO+Na}_2\text{O-K}_2\text{O}$) (A-CN-K) (fields from Gu et al., (2002)).

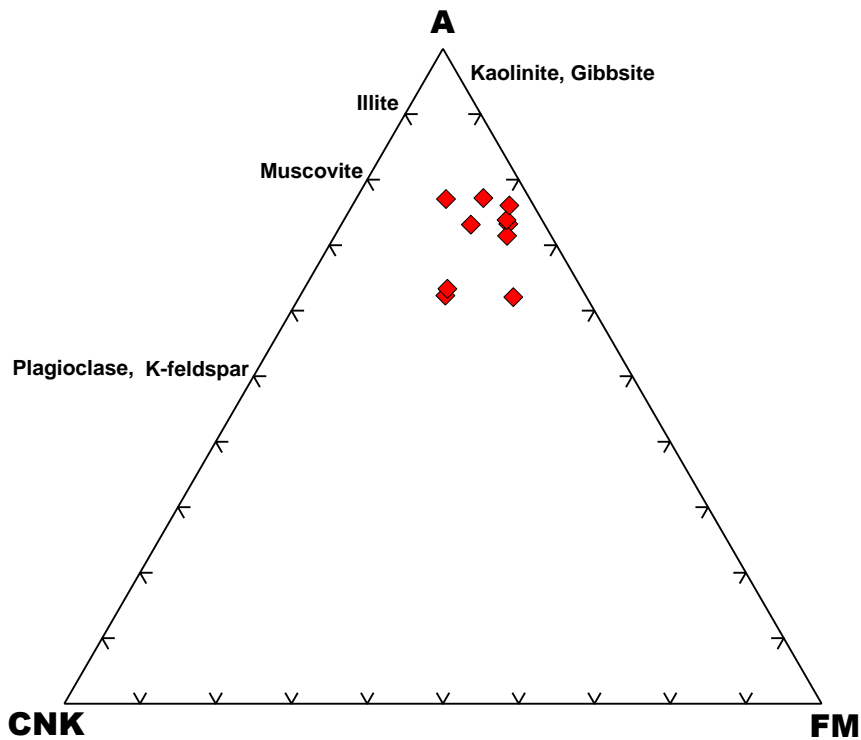


Figure 7: A–CNK–FM (Al_2O_3 — $\text{CaO}+\text{Na}_2+\text{K}_2\text{O}$ — $\text{Fe}_2\text{O}_3+\text{MgO}$) Ternary diagram of the bulk chemical composition of the Ibadan soils (after Nesbitt and Young, 1989).

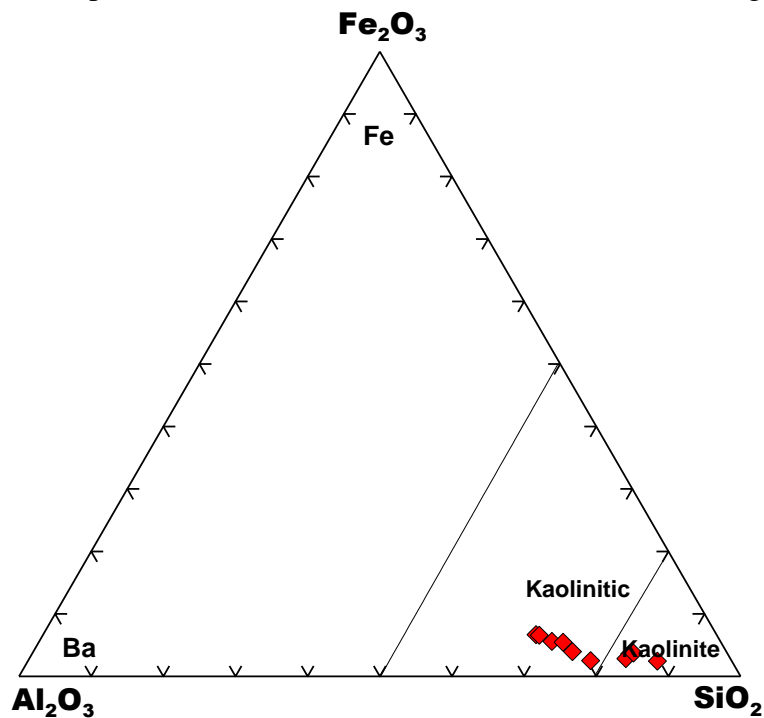


Figure 8: F–A–S (Fe_2O_3 , Al_2O_3 , SiO_2) ternary diagram, Ba = bauxitic, Fe = ferritic, Ka = kaolinite (after Schellmann, 1983).

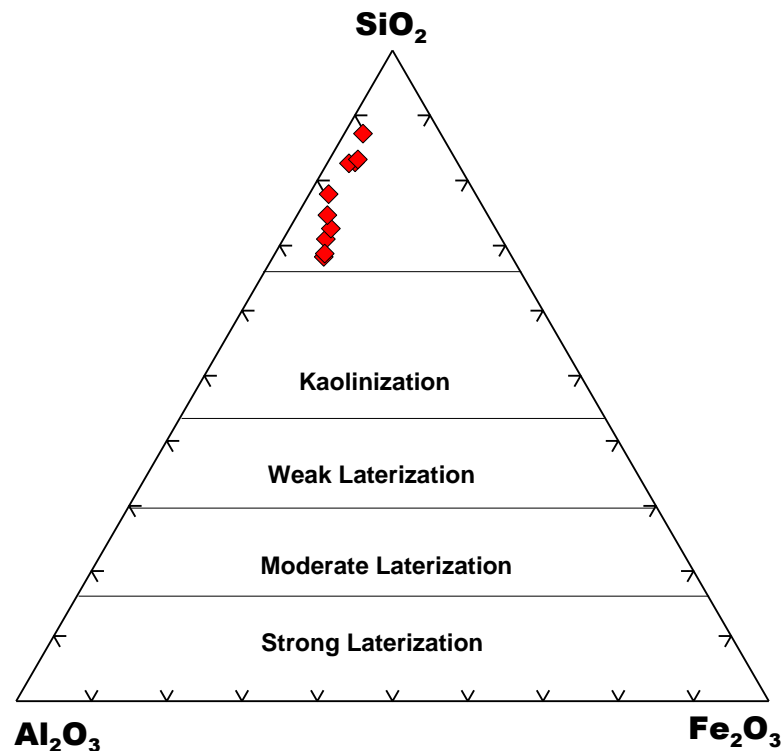


Figure 9: Extent of lateritization and weathering trend of soil samples from Ibadan (Modified after Schellmann, 1986).

Provenance

Geochemical data and their applications are important for provenance studies (Taylor and McLennan, 1985; Condie et al., 1992; Cullers, 1995). Major elements provide information on both the rock composition of the provenance and the effects of sedimentary processes, such as weathering and sorting (McLennan et al., 1993). Figure 10A, 10B and 10C are protolith discrimination diagrams utilised for the samples under investigation. Most of the samples appeared in the sedimentary/metasedimentary zone. Amphibole and quartz schist occur in association with migmatite gneiss, granitic gneiss and Pan African Older Granite bodies around Ibadan area (Okunlola, et al., 2009). The sedimentary/metasedimentary progenitor may be ascribed to these rocks. Also, the sedimentary signature may as a result of a second cycle of erosion and deposition of sediments from first cycle sediments from weathered basement rocks.

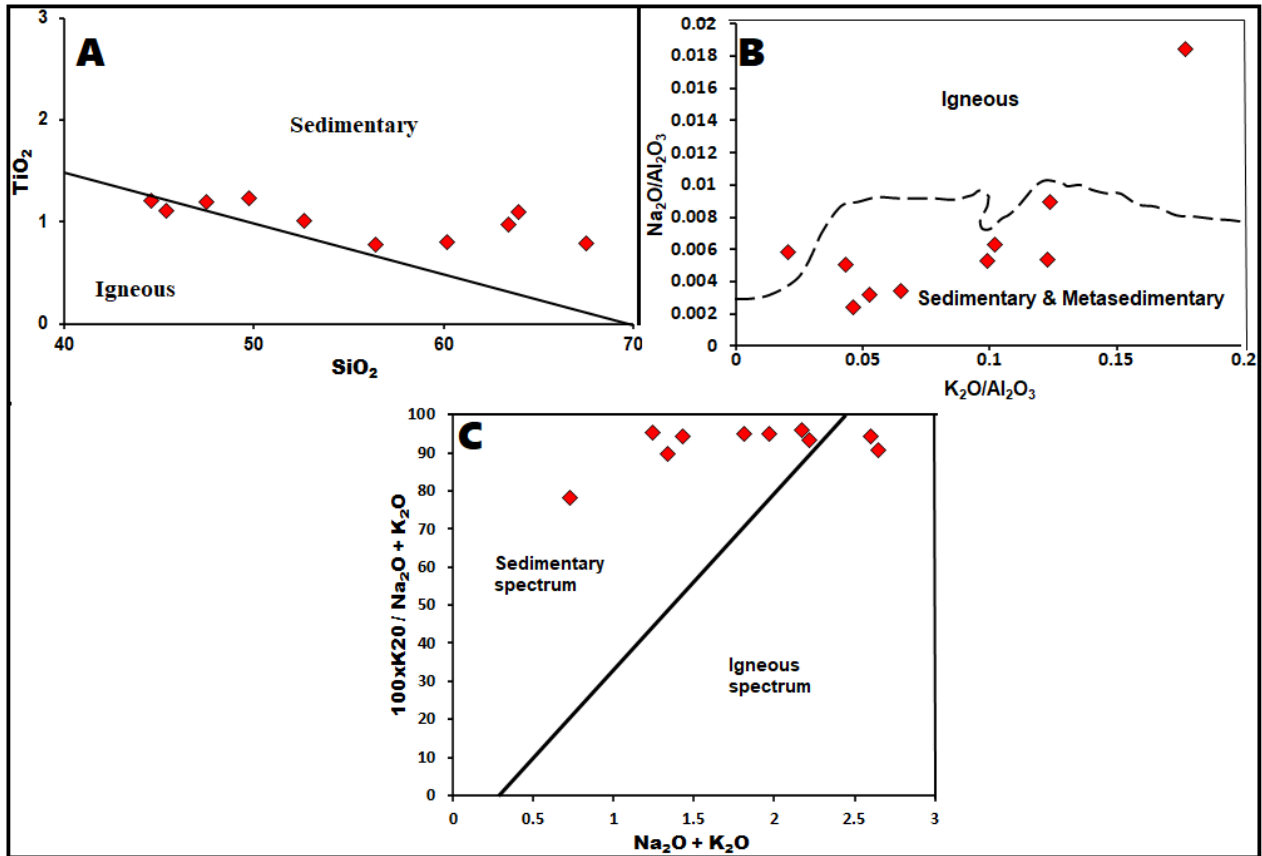


Figure 10A: $TiO_2 - SiO_2$ protolith discrimination diagram (After Tarney, 1977). B: K_2O/Al_2O_3 and Na_2O/Al_2O_3 (after Garrels and Mackenzie, 1971). C: $Na_2O + K_2O$ versus $100 \times K_2O / Na_2O + K_2O$ (after Honkamo, 1987).

Figure 11 shows that most of the samples plotted close to the granite area and towards the silica region, thus suggesting derivation from felsic sources. The plot of Na_2O versus K_2O of Figure 12 shows that most of the samples plotted in the quartz-rich zone suggesting a mixed source origin.

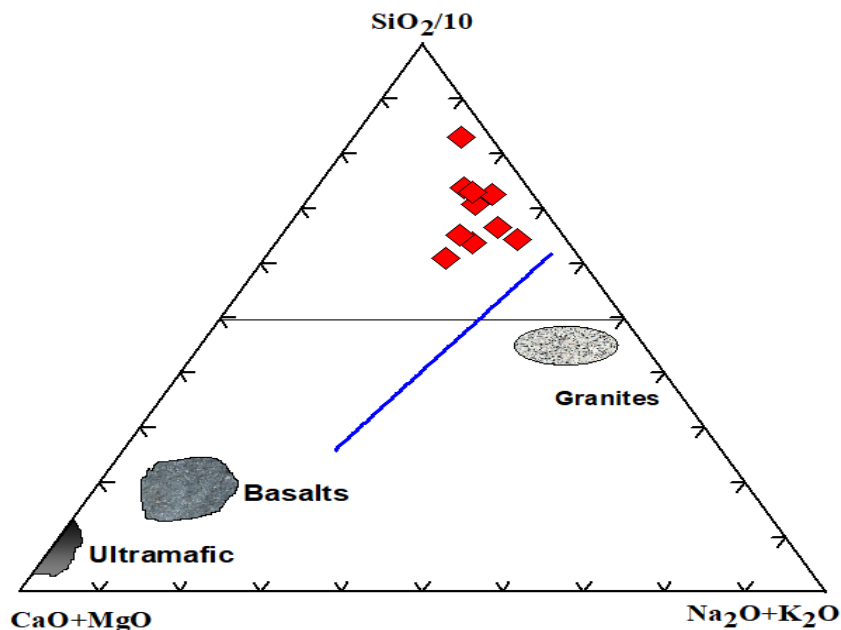


Figure 11: Plot of $Na_2O + K_2O$, $SiO_2/10$ and $CaO + MgO$ to illustrate possible affinities of the samples to felsic, mafic or ultramafic rocks (after Taylor and McLennan, 1985).

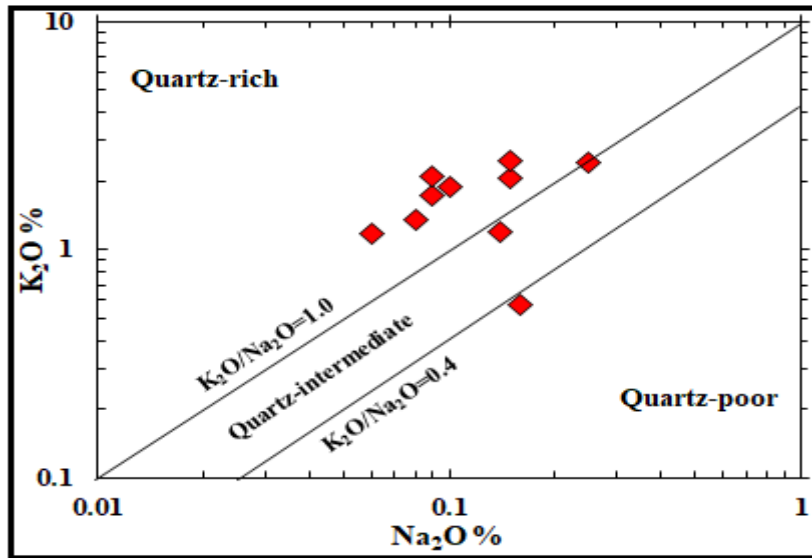


Figure 12: A bivariate plot of Na₂O versus K₂O showing quartz contents, after Crook (1974).

Zircon concentration can be applied to typify the nature and composition of source rocks and the TiO₂/Zr ratios could be used to classify source rocks as either felsic; intermediate or mafic (Hayashi, et al. (1997)). The TiO₂ versus Zr plot in Figure 13 indicated that the samples analysed plotted in both the felsic and intermediate zones, suggesting provenance from more than one source. In figure 14 all the samples plotted in the silicic area indicating that the samples are rich in silica, which also suggests a felsic source rock. A plot of K₂O against Rb in Figure 15 indicated that the studied samples are of acid/intermediate composition and they point to a source rich in felsic minerals.

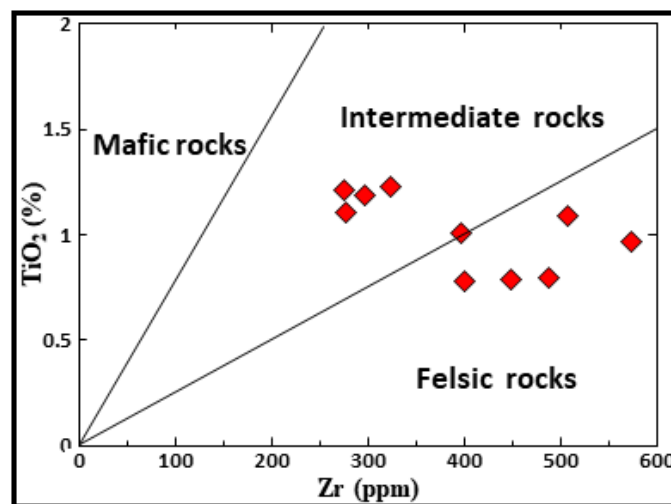


Figure 13: TiO₂-Zr plot for the sediments (Hayashi et al., 1997).

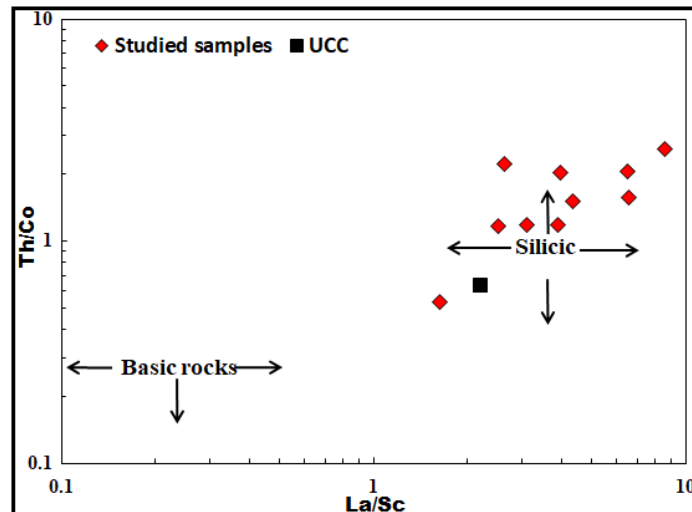


Figure 14: Th/Co versus La/Sc diagram for the samples of Nanka sandstone (Fields after Cullers, 2000).

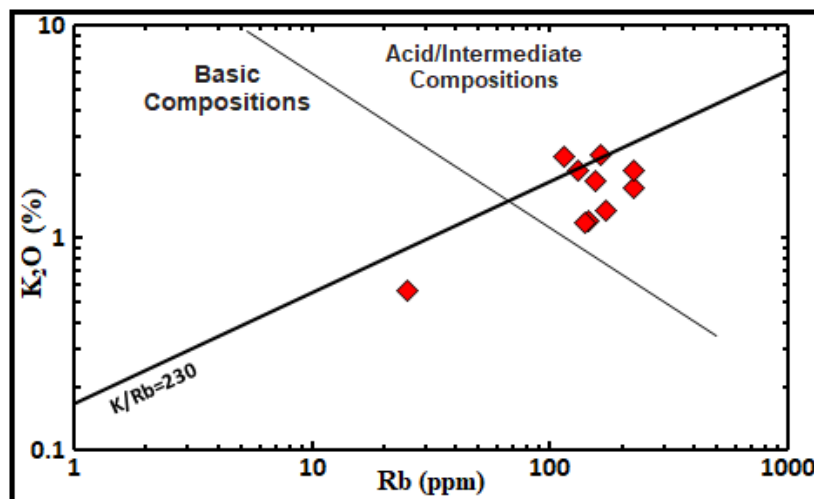


Figure 15: K₂O vs. Rb plot. Fields after Floyd and Leveridge (1987).

Paleoclimate

The degree of chemical weathering in soils increases with mean annual precipitation and mean annual temperature (Kovács et al., 2013). Using a database of major element of modern soils from Marbut (1935), Sheldon et al. (2002) developed expressions to deduce palaeo-precipitation and palaeo-temperature. Mean annual precipitation (MAP) can be connected to the chemical index of alteration without potassium (CIA–K) and is calibrated for precipitation values between 200 and 1600 mm/year (Sheldon et al. (2002):

$$\text{MAP (mm/year)} = 14.265(\text{CIA-K}) - 37.632$$

(1)

where $\text{CIA-K} = 100 \times [\text{Al}_2\text{O}_3 / (\text{Al}_2\text{O}_3 + \text{CaO} + \text{Na}_2\text{O})]$. Results obtained with this method are consistent with unconnected assessments from other proxies, such as plant fossils (Sheldon & Retallack, 2004). Kovács et al (2013) said that a climofunction by Sheldon (2006) applied to inceptisols allows mean annual temperature (MAT) to be calculated using the expression:

$$\text{MAT (}^\circ\text{C)} = 46.94C + 3.99$$

(2)

where $C = m\text{Al}/m\text{Si}$ (m is the molar ratio).

The results of the palaeo-precipitation and palaeo-temperature are shown in the Table 3.

Table 3: Paleoclimate data of the Ibadan soil samples.

Functions	D1	D2	D3	D4	D5	D6	D7	D8	D9	D10	Average
MAP (mm/year)	1275	1354	1366	1393	1384	1395	1398	1400	1386	1388	1374
MAT (°C)	12.7	10.3	17.3	13.3	23.5	21.5	12.3	20.0	23.0	19.2	17

MAP, after Sheldon et al. (2002), MAT, after Sheldon (2006).

The MAP results obtained from Equation 1 range between 1275 and 1400 ± 182 mm/year and an average of 1374 mm/year. The MAT values from Equation 2 ranged from 10.3 to 25.5 °C, with an average of 17 °C. Reconstructed paleoclimate findings based on the climofunctions (Table 3) indicate that during the formation of Ibadan soils, the climate was humid and warm. Figure 16 shows that there is correlation between MAT, MAP and CIA, suggesting that both parameters were important factors in the formation of the soil under investigation; hydrolysis appears to have greatly influenced the weathering process. We must take into consideration the impact of other effects (e.g., tectonic rejuvenation and the role of surface uplift) on the mineralogy and the CIA values (Kuhlemann et al., 2008; Varga et al., 2011).

Figures 17 and 18 are graphical paleoclimate discriminant plots based on the C-value parameter that some researchers (e.g. Zhao et al., 2007; Fu et al., 2016; Wang et al., 2017; Vd'ačný et al., 2019) have used as a proxy for climate changes. The C-value for the soil samples range between 0.41 and 3.57 with an average of 1.15. It can be deduced on the average that the paleoclimatic condition was humid. When rainfall exceeds evaporation, the ion concentrations of Ca and Mn are low enough for the elements to be deposited in low amounts, denoting a warm and humid climate, while high concentrations of Ca and Mn indicates a hot and arid climate (Cao et al., 2015). The Ca and Mn values of the soil samples are low (between 0.08-1.67 and 0.05-0.2 respectively), indicating a warm and humid climate.

The Rb/Sr ratio is a coefficient based on the differences in the resistance to weathering of micas and potassium feldspars, with which Rb is associated, and carbonates, with which Sr is associated (Gallagher and Sheldon, 2013). The Sr/Cu ratio has been applied to paleoclimatic analyses (Meng et al., 2012; Jia et al., 2013; Hu et al., 2017). Low Sr/Cu ratios indicate a warm humid climate, while high Sr/Cu ratios indicate a hot climate (Jia et al., 2013). Sr/Cu ratios between 1.3 and 5.0 denotes a warm humid climate, while Sr/Cu ratio >5.0 suggests a hot arid climate (Lerman, 1978). The Sr/Cu ratios of the soil samples range from 0.11 to 3.64 (average = 1.02) indicating that the weather was warm and humid during its deposition. According to Lerman, et al (1995), sediments with high Rb/Sr and low Sr/Cu ratios typifies warm and humid climatic conditions, while low Rb/Sr and high Sr/Cu ratios suggests hot, arid and low weathering rate climatic conditions. Data from the soils studied indicate high Rb/Sr (0.87-6.22) and low Sr/Cu (0.11-3.64) ratios, implying warm and humid climate with high weathering rate. The Ba/Sr ratio characterizes hydrothermal conditions of sedimentation, including, in particular, the leaching process (Sheldon, and Tabor, 2009; Sheldon et al., 2002). Ba is associated with potassium feldspars and is removed from the soil weaker than Sr associated with carbonates (Alekseev et al., 2019). In their work, Alekseev et al (2019) stated that the maximum Ba/Sr values (6.71 to 7.34) are characteristic of soils developed under relatively humid conditions. The Ba/Sr ratios for the soils analysed ranged between 3.36 and 9.61 (average = 6.91; maximum values from 6.99 to 9.61), which suggests a humid climatic condition

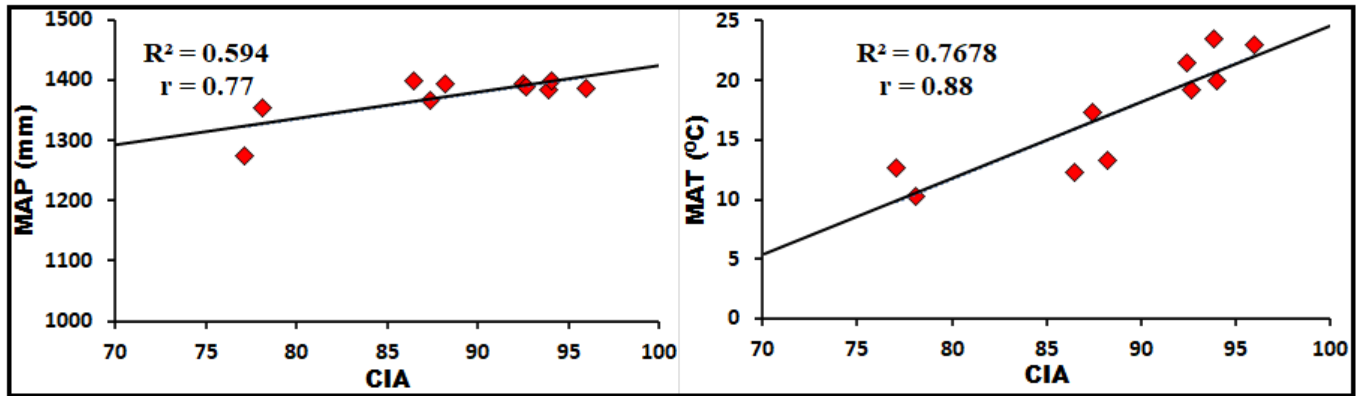


Figure 16: Relationship between mean annual temperature (MAT) and mean annual precipitation (MAP) of the studied soils.

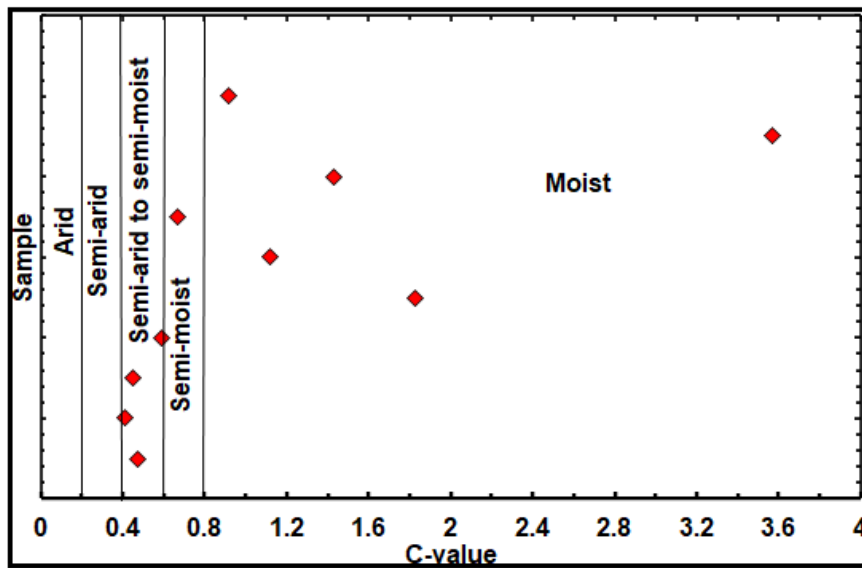


Figure 17: The C-value ($\Sigma(\text{Fe}+\text{Mn}+\text{Cr}+\text{Ni}+\text{V}+\text{Co})/\Sigma(\text{Ca}+\text{Mg}+\text{Sr}+\text{Ba}+\text{K}+\text{Na})$) of the soil samples, reflecting paleoclimate. The discriminating criteria are after Cao et al. (2012) from Hu, et al. (2016).

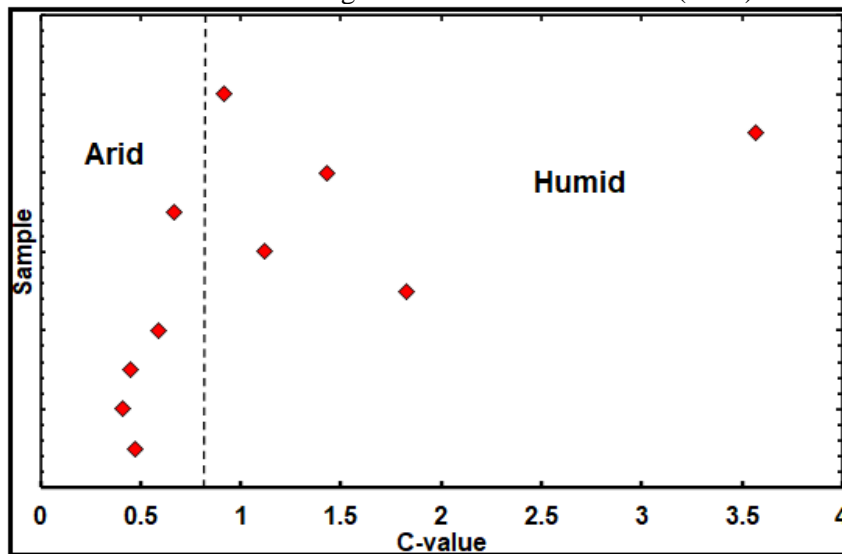


Figure 18: C-value ($\Sigma(\text{Fe} + \text{Mn} + \text{Cr} + \text{Ni} + \text{V} + \text{Co})/\Sigma(\text{Ca} + \text{Mg} + \text{Sr} + \text{Ba} + \text{K} + \text{Na})$) reflecting paleoclimate (modified by Liang et al., 2020 from Zhao et al., 2007).

CONCLUSION

The geochemistry, intensity of weathering, and paleo climatic conditions of the soils around the dumpsites at Ibadan, Oyo State, Nigeria were studied. The chemical compositions of the samples showed a relatively enriched SiO_2 (44.56-67.48) Wt. %, Al_2O_3 (13.54-27.70) and Fe_2O_3 (4.90-11.62) and strongly depleted K_2O (0.57-2.45). The oxides MgO , MnO , and Na_2O have low concentrations that are less than one (1). The low contents of these oxides are attributed to chemical destruction under oxidizing condition during weathering.

The positive correlation between Al_2O_3 and TiO_2 indicated that TiO_2 is an essential major constituent of illitic clay mineral. The positive correlation between Al_2O_3 and Fe_2O_3 shows their occurrence in clay minerals resulting from weathering of the parent rock. The positive linear trend correlation between Al_2O_3 with Fe_2O_3 and TiO_2 suggest that they occur in clay minerals formed from the weathering of granite. The ranges of CIA (81.47-96.91) and CIW (91.67-99.36) are high in the study area an indication of an intensive weathering of the parent materials. Other evidences in support of high intensity of weathering in the study area are derived from a plot of CIA against Al_2O_3 , high range of PIA (90.61- 99.32%) and the resulting low contents of CaO , K_2O and Na_2O . The relatively low concentrations of K_2O (K-feldspar), Na_2O (Na-feldspars) and an enriched aluminous clay mineral implied that the parent rocks have been exposed to an increased chemical weathering. In the area of provenance, the plot of Na_2O versus K_2O indicated a quartz-rich zone suggesting a mixed source origin whereas the TiO_2 versus Zr plot showed that the samples plotted in both the felsic and intermediate zones, suggesting provenance from more than one source. A plot of K_2O against Rb indicated that the studied samples are of acid/intermediate composition and they point to a source rich in felsic minerals. Reconstructed palaeoclimate findings based on the climofunctions indicated that during the formation of Ibadan soils, the climate was humid and warm. The Ca and Mn values of the soil samples are low (between 0.08-1.67 and 0.05-0.2 respectively), indicating a warm and humid climate. The Sr/Cu ratios of the soil samples range from 0.11 to 3.64 (average = 1.02) indicating that the weather was warm humid during its deposition. Data from the soils studied indicate high Rb/Sr (0.87-6.22) and low Sr/Cu (0.11-3.64) ratios, implying warm and humid climate with high weathering rate; the high average Ba/Sr ratio ≈ 7 also suggests a humid climatic condition.

REFERENCES

- [1] Alekseev, A.O., Kalinina, P.I. and Alekseevaa, T.V. (2019). Soil Indicators of Paleoenvironmental Conditions in the South of the East European Plain in the Quaternary Time. *Eurasian Soil Science*, 52) p. 349–358.
- [2] Bauluz, B., Mayayo, M. J., Fernandez-Nieto, C and Lopez J.M. G. (2000). Geochemistry of Precambrian and Paleozoi siliciclastic rocks from the Iberian Range N.E (Spain): Implication for source-area weathering, sorting, provenance and tectonic setting. *Chem Geol.*, 168: 135-150.
- [3] Bhatia M.R and Crook K.A.W. (1986). Trace Element characteristics of Graywackes and Tectonic Setting, Discrimination Sedimentary Basins. *Contributions to Mineralogy and Petrology*, 92, 181-193
- [4] Cao, J., Wu, M., Chen, Y., Hu, K., Bian, L., Wang, L. and Zhang, Y. (2012). Trace and rare earth element geochemistry of Jurassic mudstones in the northern Qaidam Basin, northwest China. *Chemie der Erde*, 72(3), p. 245-252.
- [5] Cao, H., Guo, W., Shan, X., Ma, L., and Sun, P. (2015). Paleolimnological environments and organic accumulation of the Nenjiang Formation in the southeastern Songliao Basin, China, *Oil Shale*, 32(1), p. 5–24.
- [6] Chen, W., and Zeng, S. (2017). Geochemical features of the black shales from the Wuyu Basin,

- southern Tibet: implications for palaeoenvironment and palaeoclimate. *Geological Journal*, 52, 282–297.
- [7] Condie K.C., Noll P.D., and Conway C.M. (1992). Geochemical and detrital mode evidence for two sources of Early Proterozoic metasedimentary rocks from the Tonto Basin Supergroup, central Arizona. *J. Sedimentary Geology*, 77, p. 51–76
- [8] Cox, R., Lowe, D.R. & Cullers, R.L. (1995). The influence of sediment recycling and basement composition on evolution of mudrock chemistry in the southwestern United States. *Geochimica et Cosmochimica Acta* 59(14): 2919–2940.
- [9] Crook K.A.W. (1974). Lithogenesis and geotectonics: The significance of compositional variation in flysch arenites (greywackes). *Society of Economical, Paleontological and Mineralogical Special Publications*, 19, p. 304–310.
- [10] Cullers R. (1995). The controls on the major- and trace-element evolution of shales, siltstones and sandstone of Ordovician to Tertiary age in wet mountains region, Colorado, USA. *Chem. Geol.* 123: 107–131.
- [11] Cullers, R.L. (2000). The geochemistry of shales, siltstones and sandstones of Pennsylvanian-Permian age, Colorado, U.S.A.: Implications for provenance and metamorphic studies, *Lithos*, 51, p. 305-327.
- [12] Fedo C.M, Nesbitt H.W, and Young G.M. (1995). Unraveling the effects of potassium metasomatism in sedimentary rocks and paleosols, with implications for paleoweathering conditions and provenance. *Geology*, 23, 921-924. [http://dx.doi.org/10.1130/0091-7613\(1995\)0232.3.CO;2](http://dx.doi.org/10.1130/0091-7613(1995)0232.3.CO;2)
- [13] Floyd, P.A., and Leveridge, B.E. (1987). Tectonic environment of the Devonian Gramscatho basin, south Cornwall; framework mode and geochemical evidence from turbiditic sandstones, *Journal of the Geological Society, London*, 144, 531–542.
- [14] Fu, X., Wang, J., Chen, W., Feng, X., Wang, D., Song, C. and Zeng, S., (2016). Elemental geochemistry of the early Jurassic black shales in the Qiangtang Basin, eastern Tethys: constraints for palaeoenvironment conditions. *Geological Journal*, 51, p. 443–454.
- [15] Gallagher, T.M. and Sheldon, N.D. (2013). A new paleothermometer for forest paleosols and its implications for Cenozoic climate. *Geology*, 41, p. 647–650.
- [16] Garrels, R.M. and Mackenzie, F.T. (1971). *Evolution of Sedimentary Rocks*. Publ. by W. W. Norton and Co. Int. New York. p394.
- [17] Gu, X.X., Liu, J.M., Zheng, M.H., Tang, J.X., and Qi, L. (2002). Provenance and Tectonic settings of the Proterozoic turbidites in Hunan, South China: Geochemical Evidence: *Journal of Sedimentary Research*, v. 72, 393– 407,
- [18] Harnois, L. (1988). The CIW index: a new chemical index of weathering. *Sedimentary Geology*.55:319-322.
- [19] Hayashi, K., Fujisawa, H., Holland, H. and Ohmoto, H. (1997). Geochemistry of ~1.9 Ga sedimentary rocks from northeastern Labrador, Canada, *Geochimica et Cosmochimica Acta*, 61(19), 4115-4137.
- [20] Honkamo, M. (1987). Geochemistry and Tectonic Setting of Early Proterozoic Volcanic Rocks in Northern Ostrobothnia, Finland. In Pharaoh, T. C., Beckinsale, R. D. and Richard D. (eds). *Geochemistry and Mineralisation of Proterozoic Volcanic Suites*, *Geol. Soc. Spec. Publ. No.*
- [21] Hu, W.Y.; Huang, B.; He, Y.; Yusef, K.K. (2016). Assessment of potential health risk of heavy metals in soils from a rapidly developing region of China. *Hum. Ecol. Risk Assess.* 22, 211–225.
- [22] Hu, J., Li, Q., Song, C., Wang, S. and Shen, B. (2017). Geochemical characteristics of the Permian sedimentary rocks from Qiangtang Basin: constraints for paleoenvironment and paleoclimate. *Terrestrial, Atmospheric and Oceanic Sciences*, 28, 271–282.
- [23] Jia, J., Liu, Z., Bechtel, A., Strobl, S.A.I. and Sun, P., (2013). Tectonic and climate control of oil shale deposition in the Upper Cretaceous Qingshankou Formation (Songliao Basin, NE China). *International Journal of Earth Sciences*, 102, 1717–1734.
- [24] Kovács, J., Raucsik, B., Varga, A., Újvári, G., Varga, G. & Ottner, F. (2013). Clay mineralogy of red clay deposits from the central Carpathian Basin (Hungary): implications for Plio-Pleistocene chemical weathering and palaeoclimate. *Turkish J. Earth. Sci.*, 22: 414-426.
- [25] Kuhlemann, J., Taubald, H., Vennemann, T., Dunkl, I. & Frisch, W. (2008). Clay mineral and

- geochemical composition of Cenozoic paleosol in the Eastern Alps (Austria). *Austrian Journal of Earth Sciences* 101, 60–69.
- [26] Lerman, A., Editor, (1978). Lakes: Chemistry, Geology, Physics. *Springer-Verlag, New York, Heidelberg, Berlin, 363p.*
- [27] Lerman, A., Imboden, D. I., Gat, J.R., Chou, L. (1995). Physics and Chemistry of Lakes. *Springer Berlin Heidelberg, 334p.*
- [28] Liang, Q., Tian, J., Zhang, X., Sun, X. and Yang, C. (2020). Elemental geochemical characteristics of Lower–Middle Permian mudstones in Taikang Uplift, southern North China Basin: implications for the FOUR-PALEO conditions. *Geosciences Journal*, 24(1), p. 17–33.
- [29] Marbut, C.F. (1935). Soils of the United States. In: O.E. Baker, editor, Atlas of American agriculture. USDA Bureau of Chemistry and Soils, U.S. Gov. *Print. Office, Washington DC.* p. 1–98.
- [30] McLennan S.M, Taylor S.R., Eriksson, K.A. (1983). Gearchean shales from the Pilbara Supergroup, Western Australian. *Geochim. Cosmochim. Acta*, 47: 1211-1222.
- [31] McLennan S.M, Taylor S.R, McCulloch M.T and Maynard, J. B (1990). Geochemical and Nd-Sr Isotopic Composition of Deep Sea Turbidites: Crustal Evolution and Plate Tectonic Associations. *Geochimimica et Cosmochimica Acta*,. 54, 2015-2050.
- [32] McLennan, S.M., Hemming, S., McDaniel, D.K., and Hanson, G.N. (1993). Geochemical approaches to sedimentation, provenance and tectonics. *Geological Society of America Special Paper* 284, p. 21–40.
- [33] Meng, Q., Liu, Z., Bruch, A.A., Liu, R. and Hu, F. (2012). Palaeoclimatic evolution during Eocene and its influence on oil shale mineralisation, Fushun basin, China. *Journal of Asian Earth Science*, 45, 95–105.
- [34] Mongelli G, Cullers R, and Muelheisen S (1996). Geochemistry of Cenozoic shales from the Varicolori Formation, Southern Apennines, Italy: implications for mineralogical, grain size control and provenance. *European Journal of Mineralogy*, 8, 733–754.
- [35] Nesbitt, H.W and Young G.M (1982). Early Proterozoic climates and plate motions inferred from major element chemistry of lutites. *Nature* 299, pp.715- 717.
- [36] Nesbitt, H.W., Young, G.M. (1989). Formation and diagenesis of weathering profiles. *J. Geol.* 97, p. 129–147.
- [37] Norman M. D, Pearson N. J, Sharma A. and Griffin W. L.(1996). Quantitative analysis of trace elements in geological materials by laser by ablation ICP-MS: instrumental operating conditions and calibration values of NIST glasses. *Geostandards Newsletter* 20, 247–261.
- [38] Norman M. D. (1998). Melting and metasomatism in the continental lithosphere: laser ablation ICP-MS analyses of minerals in spinel, herzolites from eastern Australia. *Contributions to Mineralogy and Petrology*. 130, 240- 255.
- [39] Obasi, R.A., Madukwe, H. Y and Olaosun, T. (2019). Source Area Weathering, Paleo-Environment and PaleoClimatic Conditions of Soils from Bitumen Rich Ode Irele Area of Ondo State, Nigeria. *EJERS, European Journal of Engineering Research and Science*, Vol. 4, No. 3, 59-67.
- [40] Okunlola, O.A., Adeigbe, O.C. and Oluwatoke, O.O. (2009). Compositional and petrogenetic features of schistose rocks of Ibadan area, southwestern Nigeria. *Earth sci. res. j.*, 3(2), p. 119-133. Potter, P.E. (1978). Petrology and chemistry of modern big river sands. *Journal of Geology*, 86, 423-449.
- [41] Rahaman M.A. (1976). Review of the basement geology of southwestern Nigeria, In: Kogbe, C.A. (ed.) *Geology of Nigeria. Elizabethan Publishing Company. Lagos*, 5-41.
- [42] Rahaman M.A. (1988). Recent advances in the study of the basement complex of Nigeria. In: Geological Survey of Nigeria (ed) *Precambrian Geol Nigeria*, pp 11–43.
- [43] Roser, B.P. and Korsch, R.J. (1986) Determination of tectonic setting of sandstone-mudstone suites using SiO₂ content and K₂O/Na₂O ratio. *J. Geol.* 94: 635-650.
- [44] Schellmann, W. (1983). Geochemical Principles of Lateritic Nickel Ore Formation, in Proceedings of the 2nd International Seminar on Lateritisation Processes, Sao Paulo, Brazil, 119–135.
- [45] Schellmann, W. (1986). A new definition of Laterite; In: Lateritization Processes (ed.) Banerji P K, *Geological Survey of India. Memoir*, 120, 11–17.
- [46] Sheldon, N.D. (2006). Quaternary glacial-interglacial climate cycles in Hawaii. *Journal of*

- Geology* 114, p. 367–376.
- [47] Sheldon, N.D. and Tabor, N. J. (2009). Quantitative paleoenvironmental and paleoclimatic reconstruction using paleosols. *Earth-Sci. Rev.* 95, p. 1–52.
- [48] Sheldon, N.D. & Retallack, G.J. (2004). Regional paleoprecipitation records from the Late Eocene and Oligocene of North America. *Journal of Geology* 112, p. 487–494.
- [49] Sheldon, N.D., Retallack, G.J. & Tanaka, S. (2002). Geochemical climofunctions from North American soils and application to palaeosols across the Eocene-Oligocene boundary in Oregon. *Journal of Geology*, 110, p. 687–696.
- [50] Tarney, J. (1977). Petrology, mineralogy and geochemistry of the Falkland Plateau basement rocks, site 330, deep sea drilling project. *Init. Rep.* 36, p. 893-921.
- [51] Taylor, S.R. and McLennan, S.M., 1985. The Continental Crust: Its Composition and Evolution. *Blackwell, Oxford*, 312p
- [52] Varga, A., Újvári, G. & Raucsik, B., (2011). Tectonic versus climatic control on the evolution of a loess–paleosol sequence at Beremend, Hungary: an integrated approach based on paleoecological, clay mineralogical, and geochemical data. *Quaternary International* 240, 71–86
- [53] Vd'ačný, M., Madzin, J. and Plašienka, D. (2019). Geochemical characteristics of the Upper Cretaceous to Lower Eocene sedimentary rocks from the Pieniny Klippen Belt (Western Carpathians, Slovakia): implications for tectonic setting, paleoenvironment and paleoclimate. *Geosciences Journal*, 23(5), p. 731–745.
- [54] Voicu, G., Bardoux, M., Harnois, L, and Grepeau, R. (1997). Lithological and geochemical environment of igneous and sedimentary rocks at Omai gold mine, Guyana, South America. *Exploration and Mining Geology*, 6, 153-170.
- [55] Wang, Z., Fu, X., Feng, X., Song, C., Wang, D., Chen, W., and Zeng, S., 2017. Geochemical features of the black shales from the Wuyu Basin, southern Tibet: implications for palaeoenvironment and palaeoclimate. *Geological Journal*, 52, 282–297.
- [56] Zhao, Z.Y., Zhao, J.H., Wang, H.J., Liao, J.D., and Liu, C.M. (2007). Distribution characteristics and applications of trace elements in Junggar Basin. *Natural Gas Exploration and Development*, 30, 30–33. (in Chinese with English abstract).